CURRENT DENSITY MEASUREMENTS WITH TANGENTIAL THOMSON SCATTERING IN PLASMAS WITH PEAKED AND HOLLOW TEMPERATURE PROFILES

F.A. Karelse, C.J. Barth, M.N.A. Beurskens, G.M.D. Hogeweij, N.J. Lopes Cardozo, H.J. van der Meiden and the RTP team

FOM-Instituut voor Plasmafysica 'Rijnhuizen', Association Euratom-FOM, Trilateral Euregio Cluster, P.O.Box 1207, 3430 BE Nieuwegein, The Netherlands

Introduction. The research at the Rijnhuizen Tokamak Project (RTP; $I_p \leq 150$ kA, $B_T \leq 2.5$ T, $R/a = 0.72/0.164$ m) focuses on electron transport. In this paper tangential Thomson scattering measurements of the current density (j) profile are presented for on- and off-axis Electron Cyclotron (EC) heated plasmas. Recently, it has been shown that for a scan of the deposition radius ($\rho_{\rm dep}$) of the EC Heating (ECH) the electron temperature (T_e) profiles fall into distinct classes separated by sharp transitions [1,2]. In this paper j profile measurements corresponding to these T_e profile classes will be given and compared with calculations based on neo-classical resistivity. According to these calculations the minima of the safety factor fall into half integer bands.

Tangential TS. The tangential TS diagnostic measures the light scattered from a vertically injected ruby laser ($\lambda_0 = 694.3$ nm, $E \leq 25$ J) along a chord of 60% of the plasma diameter, see Fig. 1 [3,4]. The spatial resolution is ~ 1.5 % of a, the wavelength resolution is 2.5 nm for the interval between 550 and 800 nm. The double detector allows for a plasma light measurement for correction of the scattered signal. The details of the tangential TS diagnostic are to be published in a separate paper.

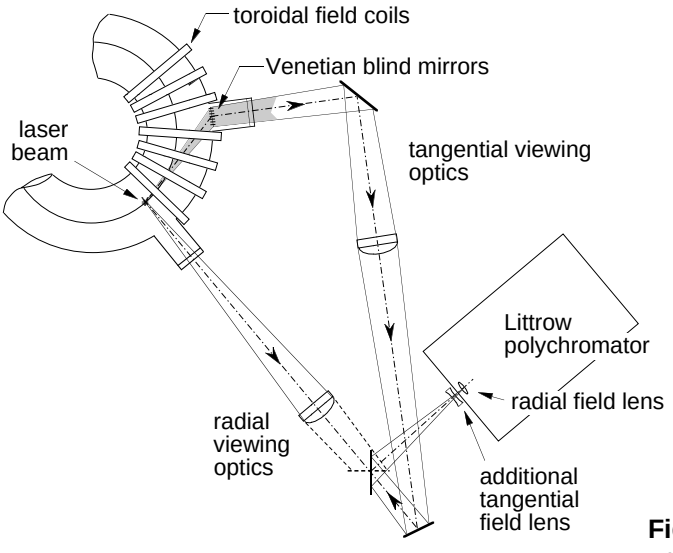

Fig. 1. Top view of the RTP Thomson scattering system.

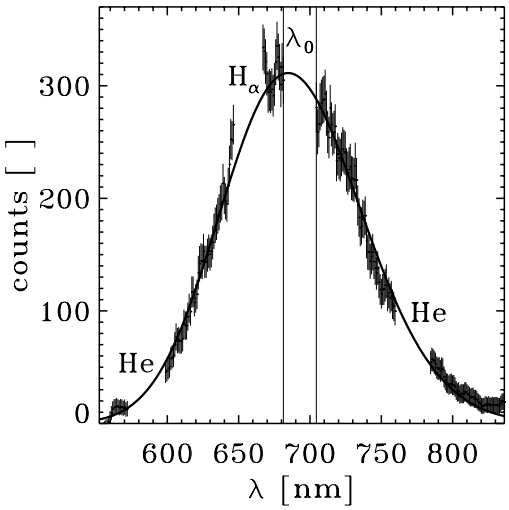

Fig. 2. Typical summed spectrum of discharges with central ECH. The Helium and H_α lines are cut out as indicated. The line is the fit to the data, giving $T_e = 1321$ eV and $\Delta\lambda = 2.9$ nm.

The tangential set-up measures T_e and the electron density (n_e) with an error of 5 % and 3 % respectively. Since the scattered light is collected horizontally under a small angle of 17° with the toroidal axis, the observed spectrum is Doppler shifted. This shift ($\Delta\lambda$) is due to the drift velocity (v_d) and the ion velocity (v_i). v_d is proportional to j and $1/n_e$. Typical value of

$\Delta\lambda$ is 1 nm with a statistical error of 100%. The error is reduced to below 10 % by averaging 10 z-positions and 15 discharges. Furthermore, to correct for systematic deviations of the shift, discharges with positive and negative current are compared.

Data analysis. The spectrally resolved laser chord image is projected onto a CCD camera (385x512 pixels). Each pixel is one fourth of the wavelength resolution wide and one third of the z resolution high. The laser frequency is cut out optically, the H-alpha and He lines are cut out numerically, see Fig. 2. Relative calibration is done by comparison with the known spectrum of a Tungsten band lamp. The absolute calibration is done by comparison with the known quantity of Rayleigh scattered photons [3].

The Mattioli distribution [5] is fit to the spectra revealing three parameters: The width, the amplitude and the shift ($\Delta\lambda$). The statistical error on $\Delta\lambda$ is deduced from the reduced χ^2 test of the fit. To improve this the CCD images are added before fitting. To reduce systematic deviations discharges of positive and negative current are compared.

The current density follows from $j = n_e e v_d$ where $v_d = c\Delta\lambda/\lambda_0 + v_i$, c is the velocity of light, λ_0 the laser wavelength and v_i the ion rotation frequency. The error on j is dominated by the error on $\Delta\lambda$. Since the absolute value of this error is almost independent of $\Delta\lambda$, the relative error on j increases as j decreases. The safety factor profile $q(r)$ is obtained by surface integration of $j(r)$. Due to the integration the error on q tends to decrease towards the edge.

The laser misses the center of the flux surfaces due to the Shafranov shift (δ). δ is estimated 1.0 ± 1 cm. For T_e profiles which are flat in the center, j is assumed flat too, and q has been corrected by assuming $\delta = 1$ cm. The remaining uncertainty decreases with r as $1/r^2$.

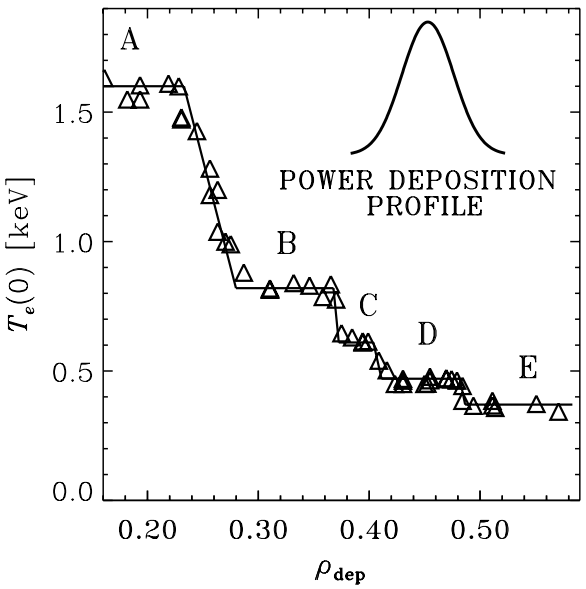

Fig. 3. The central electron temperature as a function of the deposition radius. The line is a guide for the eye.

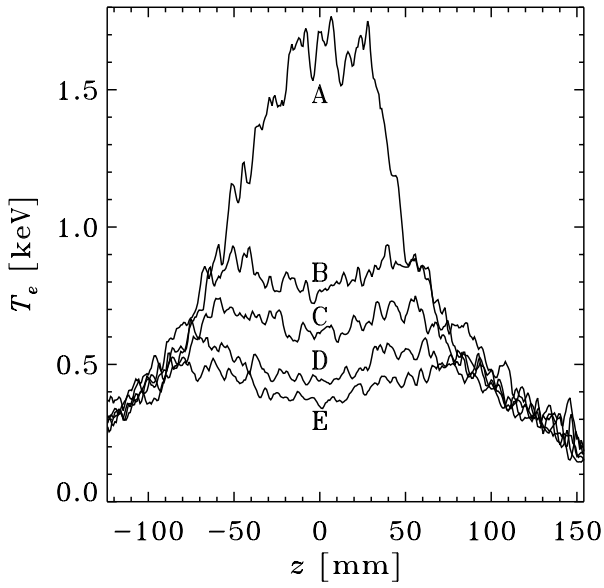

Fig. 4. Typical electron temperature profiles corresponding to the plateaus in Fig. 3.

Plasma rotation. The obtained Doppler shift is to be corrected for v_i to yield v_d. There is no direct measurement of v_i in the center. A grazing incidence spectrometer [6] gives the position of a carbon line (656.28 nm) stemming from the edge region, which yields an ion temperature $T_i \sim 17$ eV and $v_i = 3 \pm 1 \cdot 10^3$ m/s, opposite to the electron drift velocity. We

assume that $v_i \propto \sqrt{T_i}$ and has a linear profile shape. For a typical $T_i(0)$ of 400 eV this gives $v_i(0) = 15 \pm 5 \cdot 10^3$ m/s, which is only 2.5 % of $v_d(0)$ for ohmic discharges.

Deposition scan. In Fig. 3 the central T_e is given as a function of $\rho_{\rm dep}$ of a set of discharges for which the toroidal magnetic field was varied between 2.0 and 2.25 T, i.e. $\rho_{\rm dep}$ varied from 0 to 0.56. The steps are labeled A to E and all data in this paper will be labeled correspondingly. In Fig. 4 the T_e profiles of the plateaus of Fig. 3 are shown.

Current density. In Fig. 5 the j profiles for the profiles labeled A to D are shown as measured with tangential TS. For comparison also the j profiles are given calculated from $T_e(r)$ assuming neo-classical resistivity, corrected for bootstrap current. In Fig. 6 the corresponding safety factor (q) profiles are shown, together with the q profiles from the calculation. These profiles are more clearly separated, because of the integration involved in deriving q. The measurements indicate a negative central shear region for the profiles B to D.

A few unexpected features of the measurements call for attention:

1) The j profiles show asymmetry with respect to $z = 0$ outside error bars.
2) The profiles B, C and D have a high q_0.
3) q profile A is low in the region between 60 and 90 mm.

The cause for these systematic deviations is presently not understood.
Ad. 3) The current running within the surface of the outermost measurement equals the total current. For the profiles B, C and D this percentage is 60, 50 and 43, respectively. The calculations vary only between 50 and 75 %.

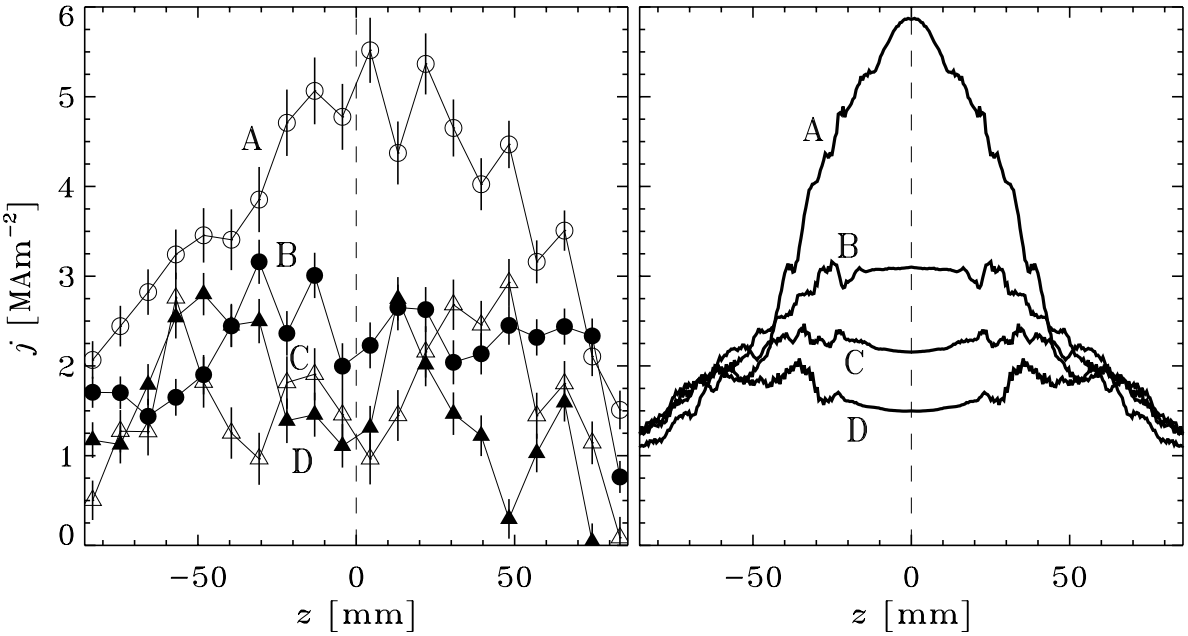

Fig. 5. j as measured with tangential TS (left) and as calculated based on neo-classical resistivity (right) corresponding to the T_e profiles of Fig. 4 marked with A to D.

Apart from the deviations mentioned before, the agreement between the measurements and the calculations is rather good, especially in the region of the respective deposition radii. This holds inside $\rho_{\rm dep}$ too, regarding the increasing uncertainty on the calculations towards the axis in these regions.

Note that according to Fig. 6 both the measurements and the calculations show that the minimum values of q ($q_{\min}$) are ordered in half integer bands for these four profiles, see Fig. 7. The calculated $q_{\min}$ value for the fifth profile E is 3.25, completing the order.

The measurements show that for the profiles A to D, j changes according to the expectations from neo-classical resistivity. Furthermore, the ordering of $q_{\min}$ into half integer bands provides a firmer basis for the transport model, presented in [7]. This models main assumption is the existence of a set of transport barriers near half integer q-values. It reproduces not only the deposition scan as presented in Fig. 3, within error bars, it also reproduces the T_e profiles of Fig. 4.

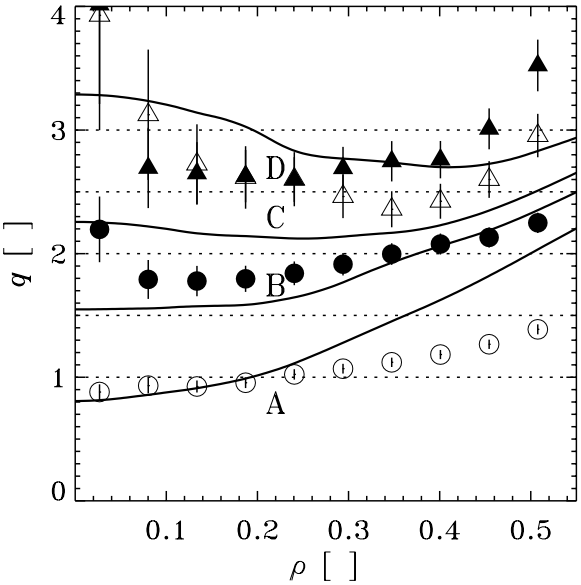

Fig. 6. q profiles corresponding to the j profiles of Fig. 5.

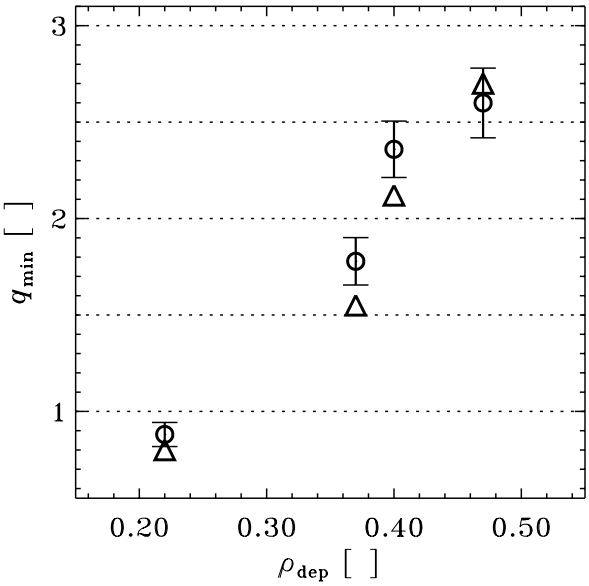

Fig. 7. q_{min} as a function of ρ_{dep} for the measurements (○) and for the neo-classical calculations (△).

Conclusion. Tangential TS j measurements of on- and off-axis EC heated plasmas have been presented. The T_e profiles fall into distinct classes as a function of the power deposition radius $\rho_{\rm dep}$ and the j profiles corresponding to those classes are determined. The j profiles confirm the results of neo-classical calculations from the T_e profiles. Data and calculations both indicate that the minimum value of q of these profiles is ordered in half integer bands. This confirms the assumed transport model linking transport barriers to half integer values.

Acknowledgements. The authors wish to thank D. Badoux, R.M. Gravestijn and F.G. Meijer for their input in analyzing the spectrometer data. This work was performed as part of the research program of the association agreement Euratom-FOM with financial support from NWO and Euratom.

References

[1] N.J. Lopes Cardozo et al.: Plasma Phys. Control. Fusion **39**, B303-B316 (1997).
[2] M.R. de Baar et al.: *Proc. 24th EPS Conf. Control. Fusion Plasma Phys.*, PII.585 (1997).
[3] C.J. Barth et al.: Rev. Sci. Instrum. **68**, 3380 (1997).
[4] M.N.A. Beurskens et al.: Rev. Sci. Instrum. **68**, 721 (1997).
[5] M. Mattioli: EUR-CEA-FC-752 (1975).
[6] F.G. Meijer et al.: *Proc. 24th EPS Conf. Control. Fusion Plasma Phys.*, PII.609 (1997).
[7] A.M.R. Schilham et al.: *this conference.*